

Recurrent generation of maximally entangled single-particle states via quantum walks on cyclic graphs

Dinesh Kumar Panda¹* and Colin Benjamin²†

School of Physical Sciences, National Institute of Science Education and Research Bhubaneswar, Jatni 752050, India and Homi Bhabha National Institute, Training School Complex, Anushaktinagar, Mumbai 400094, India

 (Received 12 January 2023; revised 14 June 2023; accepted 14 August 2023; published 25 August 2023)

Maximally entangled single-particle states (MESPS) are opening new possibilities in quantum technology, as they have the potential to encode more information and are robust to decoherence compared to their nonlocal two-particle counterparts. We find that a single coin can generate MESPS at recurrent time steps (periodically) via discrete-time quantum walks on both 4- and 8-site cyclic graphs. This scheme is resource saving, with possibly the most straightforward experimental realization since the same coin is applied at each time step. We also show that recurrent MESPS can be generated on any arbitrary k -site cyclic graph, $k \in \{3, 4, 5, 8\}$ via effective-single (identity and arbitrary coin) or two-coin evolution sequences. Beyond their use in fundamental research, we propose an application of the generated MESPS in quantum cryptography protocols. MESPS as cryptographic keys can strengthen quantum-secure communication.

DOI: [10.1103/PhysRevA.108.L020401](https://doi.org/10.1103/PhysRevA.108.L020401)

Introduction. Hybrid or single-particle entanglement (SPE) refers to the entanglement between different degrees of freedom such as spatial mode, polarization, and orbital angular momentum belonging to the same particle [1]. The quantum signature of SPE is contextuality, which rules out realistic noncontextual hidden-variable theories and violates Bell's inequality. Though SPE lacks in nonlocality, it has its significance plus advantages over the nonlocal or multiparticle entanglement [1,2]. SPE enables encoding more information at the single-particle level, is more robust against decoherence, and has simpler experimental implementation than its nonlocal bipartite counterpart [1,3,4]. SPE has significant applications in photonic quantum information processing and analysis of states of photons and elementary particles [1]. Since an entangled state can be transmitted employing a single particle, SPE is a proven resource to improve existing QKD (quantum key distribution) protocols like the BB84 for secret key sharing and a QKD scheme with single-particle entangled photons, see [1,5]. Quantum joining, a physical process that allows the transfer of interparticle entanglement between photons into a single output photon's hybrid entanglement and its inverse, has been reported, and it has applications in quantum networking [6]. Photonic SPE states are potentially advantageous in optical quantum networks because they enable a more flexible network with every photon transmitted via a suitable channel [7]. SPE has also been used in experimental tests of noncontextual hidden-variable theories [1].

A quantum walker (or particle) is represented by a wave function and obeys the quantum superposition principle, and this makes quantum walks (QWs) superior compared to their

classical counterparts [8]. A discrete-time quantum walk (DTQW) evolves by repeatedly applying two quantum operators: coin and shift. A quantum walk can be described on a one- or two-dimensional (1D, 2D) lattice and analogously on a cyclic graph with k sites (k cycle). For some detailed studies on QWs on k cycles, see Refs. [9–11]. Reference [11] reports on the experimental implementation of QW on cyclic graphs with photons using linear optical elements. A recent work [12] shows that it is possible to design an ordered or periodic QW by combining two chaotic QWs on 3- or 4-cycle via the Parrondo strategy [13]. Intriguingly, the emergence of order from chaos and its inverse in QWs has applications in quantum cryptography [12], quantum-secure direct communication protocols [14], and in developing a theory of quantum chaos control [15].

Several manuscripts recently reported that DTQWs on 1D lines could be efficient tools to generate entangled single-particle states (SPS) or SPE, see Refs. [3,4,16–21]. Refs. [4,17] report on the experimental realization of SPE generation. Reference [16] shows that by incorporating Parrondo sequences of coin operators in 1D DTQWs one can obtain phase-independent SPE and, in a particular case, maximal SPE independent of the initial state parameters for time steps of 3 and 5.

There has been no attempt to generate maximally entangled SPS (MESPS), and for that matter, SPE in cyclic graphs. Also, seeing the versatility of DTQWs and the preeminent applicability of SPE, exploring different methods to generate highly or maximally entangled SPS via DTQWs is an important task, as it would contribute to extending the horizons of quantum technologies [1]. Our main aim in this work is to study the propensity of DTQWs on cyclic graphs in generating MESPS using a single coin. In addition, we also study MESPS generation using an effective-single coin (i.e., coin operator and identity operator) or two coins in a deterministic

*dineshkumar.quantum@gmail.com

†colin.nano@gmail.com

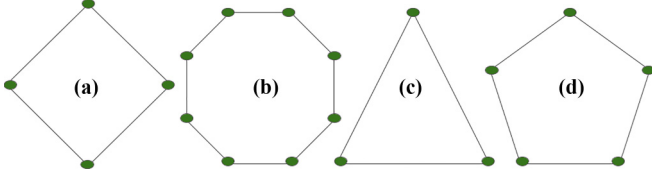


FIG. 1. 4-cycle (a) and 8-cycle (b), 3-cycle (c) and 5-cycle (d), with sites marked by green dots.

evolution-operator sequence and their relation to ordered QW dynamics.

DTQW on cyclic graphs. A DTQW on a k cycle (Fig. 1) is defined on a tensor product space (H) of position (H_P) and coin (H_C) Hilbert spaces, i.e., $H = H_P \otimes H_C$. H_C is defined on the computational basis $\{|0_c\rangle, |1_c\rangle\}$, whereas H_P has the computational basis $\{|x_p\rangle : x_p \in \{0, 1, 2, \dots, k-1\}\}$. If the quantum walker is initially localized at the site $|0_p\rangle$ in a general superposition of the coin states, it is represented by $|\psi_i\rangle$ or $|\psi(t=0)\rangle$, i.e.,

$$|\psi(t=0)\rangle = \cos\left(\frac{\theta}{2}\right)|0_p, 0_c\rangle + e^{i\phi} \sin\left(\frac{\theta}{2}\right)|0_p, 1_c\rangle, \quad (1)$$

with $\theta \in [0, \pi]$ and $\phi \in [0, 2\pi)$. The unitary coin operator is

$$\hat{C}_2(\rho, \gamma, \eta) = \begin{pmatrix} \sqrt{\rho} & \sqrt{1-\rho}e^{i\gamma} \\ \sqrt{1-\rho}e^{i\eta} & -\sqrt{\rho}e^{i(\gamma+\eta)} \end{pmatrix}, \quad (2)$$

where $0 \leq \rho \leq 1$ and $0 \leq \gamma, \eta \leq \pi$.

The walker moves to the left (right) by one site for coin state $|0_c\rangle$ ($|1_c\rangle$). For the walker on k cycle, we use the shift operator $\hat{S} = \sum_{q=0}^1 \sum_{j=0}^{k-1} |((j+2q-1) \bmod k)_p\rangle \langle j_p| \otimes |q_c\rangle \langle q_c|$. The full evolution can be expressed as

$$U_k(t) = \hat{S} \cdot [I_k \otimes \hat{C}_2(\rho(t), \gamma(t), \eta(t))], \quad (3)$$

where I_k is a $k \times k$ identity matrix. The time evolution of the system (quantum walker) after t time steps is then

$$\begin{aligned} |\psi(t)\rangle &= U_k(t)|\psi(t-1)\rangle = U_k(t)U_k(t-1)\dots U_k(1)|\psi(0)\rangle, \\ &= \sum_{j=0}^{k-1} [\alpha_0(j, t)|j_p, 0_c\rangle + \alpha_1(j, t)|j_p, 1_c\rangle], \end{aligned} \quad (4)$$

where $\alpha_0(j, t)$ and $\alpha_1(j, t)$ are amplitudes for the states $|j_p, 0_c\rangle$ and $|j_p, 1_c\rangle$, respectively.

Measuring entanglement. The initial quantum state in Eq. (1) is pure and separable, and it evolves unitarily via DTQW. We use entanglement entropy (E) to quantify the entanglement between the coin and position degrees of freedom of the time-evolved quantum state $|\psi(t)\rangle$ [22]. Let ρ_ψ be density operator for $|\psi(t)\rangle$ i.e., $\rho_\psi = |\psi(t)\rangle \langle \psi(t)|$ and reduced density operator (ρ_c) for the coin space is, $\rho_c \equiv \text{Tr}_p(\rho_\psi)$, where the partial trace Tr_p is taken over the position degrees of freedom. The eigenvalues of the reduced density matrix ρ_c are, $E_\pm = \frac{1}{2} \pm |\vec{n}|$, with $\vec{n} = (\Re(\sum_j \alpha_1(j, t)\alpha_2^*(j, t)), \Im(\sum_j \alpha_1(j, t)\alpha_2^*(j, t)), \frac{1}{2} \sum_j (|\alpha_1(j, t)|^2 - |\alpha_2(j, t)|^2))$. The entanglement entropy E is the von Neumann entropy for the coin state's reduced density matrix ρ_c . E is defined as $E(\rho_c) = -\text{Tr}(\rho_c \log_2 \rho_c)$, with 0 for separable states and 1 for MESPS, and can be calculated via $E = -E_- \log_2 E_- - E_+ \log_2 E_+$.

To check whether our results are correct, we also calculate the Schmidt norm (another entanglement measure), which is given by $S = \sqrt{E_-} + \sqrt{E_+}$, and for the present system with $\min(\dim H_P, \dim H_C) = 2$, S for a MESPS is $\sqrt{2}$ [3, 16]. In the Supplemental Material (SM) [23] Sec. II, we show results from both the entanglement measures and their similar nature.

Periodicity of DTQW on cyclic graphs. Further, the QW on a k cycle is said to be ordered or periodic if the walker reverts to its initial state after a time step, say $t = N$, irrespective of the initial quantum state. For an ordered QW with period N , we may write

$$|\psi(N)\rangle = U_k(N)U_k(N-1)\dots U_k(1)|\psi_i\rangle = |\psi_i\rangle. \quad (5)$$

If we apply the same coin at each time step in the above QW evolution, i.e., $U_k(t) = U_k(t-1) = \dots U_k(1) = U_k$ (say), then Eq. (5) is equivalent to $U_k^N|\psi_i\rangle = \sum_{i=1}^{2k} a_i \lambda_i^N |\lambda_i\rangle$, wherein the arbitrary $|\psi_i\rangle$ is expressed in terms of the eigenvalues $\{\lambda_i\}$ and eigenvectors $\{|\lambda_i\rangle\}$ of U_k , i.e., $|\psi_i\rangle = \sum_{i=1}^{2k} a_i |\lambda_i\rangle$. From Eq. (5) the condition of periodicity for the QW follows: $U_k^N = I_{2k}$ or $\lambda_i^N = 1$, $\forall i \in \{1, 2, \dots, 2k\}$. Any unitary evolution operator which satisfies this condition gives a periodic probability distribution for the walker's position and yields ordered QW. Otherwise, the QW is said to be chaotic. Furthermore, to simplify the problem of finding the eigenvalues of U_k and hence the periodicity of the QW, the 2×2 block circulant matrix U_k is block diagonalized by using a commensurate Fourier matrix tool as done in Ref. [9]. Then the block-diagonalized form of U_k is given by $F_c U_k F_c^\dagger = \text{diag}[U_{k,0}, U_{k,1}, \dots, U_{k,k-1}]$, wherein $F_c = F^k \otimes F^2$ with F^M (with $M \in \{k, 2\}$) being an $M \times M$ commensurate Fourier matrix, i.e., $F^M = (F_{m,n}^M) = \frac{1}{\sqrt{M}} (e^{2\pi i \frac{mn}{M}})$, where $m, n = 0, 1, \dots, M-1$. The periodicity condition is satisfied if the eigenvalues $\lambda_{k,l}^\pm$ of each block $U_{k,l}$ satisfy the condition, $(\lambda_{k,l}^\pm)^{\frac{N}{v}} = 1$, where v is the number of steps in the evolution-operator sequence which repeat. In Refs. [9, 10], examples of parameter values for U_k to obtain ordered QWs have been given. We discuss an analytical approach for obtaining values of such parameters, viz. $\{\rho, \gamma, \eta\}$ yielding recurrent MESPS via ordered QWs, with various evolution-operator sequences in the *Results* section.

Results. MESPS with single-coin evolution sequences. A general framework for any single coin $\hat{C}_2(\rho, \gamma, \eta)$ to yield MESPS at time step $t = 1$ for the QW on any k cycle via the single-coin evolution sequence $A_k A_k A_k \dots$ with evolution operator $A_k = U_k(\rho, \gamma, \eta) = \hat{S} \cdot [I_k \otimes \hat{C}_2(\rho, \gamma, \eta)]$ is established in the SM Sec. I [23]. A single coin of the form

$$\hat{C}_2\left(\rho = \frac{1}{2}, \gamma, \eta\right) = \frac{1}{\sqrt{2}} \begin{pmatrix} 1 & e^{i\gamma} \\ e^{i\eta} & -e^{i(\eta+\gamma)} \end{pmatrix}, \quad (6)$$

under the constraint $(\gamma + \phi) \in \{\frac{\pi}{2}, \frac{3\pi}{2}\}$, generates MESPS at $t = 1$ for any odd or even cycle, or a line, from an arbitrary separable initial state Eq. (1). In addition, a subset of such arbitrary single coins, i.e., $\hat{C}_2(\rho = \frac{1}{2}, \gamma \in [0, \pi], \eta \in [0, \pi])$, with parameters $(\gamma + \eta) \in \{0, \frac{\pi}{2}, \pi, \frac{3\pi}{2}\}$, yields recurrent or periodic MESPS (starting at time step $t = 1$) on both 4-cycle and 8-cycle, see SM Sec. I [23].

Initial states [Eq. (1)] having arbitrary $\phi \in [0, 2\pi)$ values like $\phi = \frac{\pi}{6}, \frac{\pi}{5}, \frac{\pi}{4}, \frac{\pi}{3}, \frac{\pi}{2}, \pi$, etc. can generate MESPS

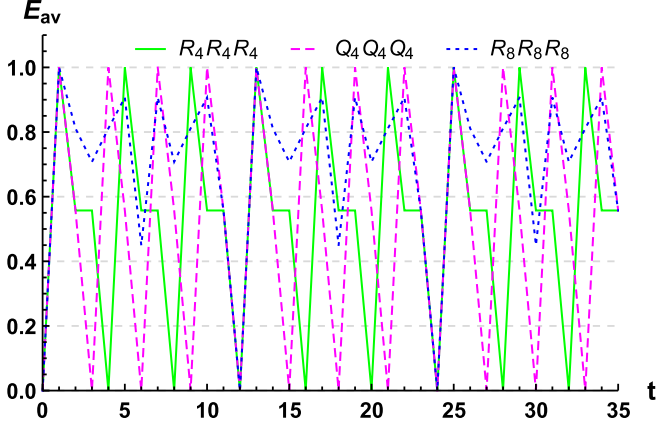


FIG. 2. E_{av} vs time steps (t) for single-coin evolution sequences: $R_4R_4R_4\dots$ (solid green), $Q_4Q_4Q_4\dots$ (dashed magenta) for 4-cycle, and $R_8R_8R_8\dots$ (dotted blue) for 8-cycle, and an arbitrary separable initial state with $\phi = \frac{\pi}{6}$.

recurrently on both 4- and 8-cycles. For example, see Fig. 2, where the single-coin evolution sequence $R_kR_kR_k\dots$, with $R_k = U_k(\rho = \frac{1}{2}, \gamma = \frac{\pi}{3}, \eta = \frac{2\pi}{3}) = \hat{S} \cdot [I_k \otimes \hat{C}_2(\rho = \frac{1}{2}, \gamma = \frac{\pi}{3}, \eta = \frac{2\pi}{3})]$, yields recurrent MESPS on both $k = 4$ -cycle and $k = 8$ -cycle, for the initial state with $\phi = \frac{\pi}{6}$. Note that each data point in Fig. 2 (and in the following figures) is an average of the entanglement entropy (E_{av}), and the average is taken over θ with the mentioned ϕ value and is evaluated as $E_{av} = \frac{1}{\pi} \int_0^\pi E d\theta$. For MESPS, $E_{av} = 1$. The sequence $R_4R_4R_4\dots$ at $t = 1, 5, 9, \dots$ yields MESPS on 4-cycle, with period 4, whereas the sequence $R_8R_8R_8\dots$ yields MESPS at $t = 1, 13, 25, \dots$ (with period 12) on 8-cycle. Here the coin $\hat{R} = \hat{C}_2(\frac{1}{2}, \frac{\pi}{3}, \frac{2\pi}{3})$, which is applied at each QW time step, is involutory i.e., $\hat{R}^2 = I_2$. However, the use of involutory coins is not a necessary condition to generate recurrent MESPS; for instance, the single noninvolutory coin evolution sequence $Q_4Q_4Q_4\dots$ with $Q_4 = U_4(\frac{1}{2}, \frac{\pi}{3}, \frac{\pi}{6})$ (i.e., an noninvolutory coin $\hat{Q} = \hat{C}_2(\rho = \frac{1}{2}, \gamma = \frac{\pi}{3}, \eta = \frac{\pi}{6})$ with $\hat{Q}^2 \neq I_2$, applied at each time step) on 4-cycle, yields MESPS with period 3 at $t = 1, 4, 7, 10, \dots$ (see, Fig. 2), for the same initial state.

By considering another separable initial state Eq. (1) with $\phi = \pi$, we find that noninvolutory Fourier coin $\hat{F} = \hat{C}_2(\frac{1}{2}, \frac{\pi}{2}, \frac{\pi}{2})$, via its single-coin evolution sequence $F_kF_kF_k\dots$ with $F_k = U_k(\frac{1}{2}, \frac{\pi}{2}, \frac{\pi}{2})$, yields recurrent MESPS on both $k = 4$ - and $k = 8$ -cycles, as shown in Fig. 3. The sequences $F_4F_4F_4\dots$ and $F_8F_8F_8\dots$ generate MESPS respectively at $t = 1, 5, 9, 13, \dots$ with period 4 and at $t = 1, 13, 25, \dots$ with period 12. Again, for $\phi = \pi$, the involutory single-coin evolution sequence $H_4H_4H_4\dots$ with $H_4 = U_4(\frac{1}{2}, 0, 0)$ [i.e., Hadamard coin $\hat{H} = \hat{C}_2(\rho = \frac{1}{2}, \gamma = 0, \eta = 0)$ applied at each time step] on 4-cycle yields MESPS (with period 4) at $t = 2, 6, 10, \dots$ (since $\gamma + \phi = \pi$), as shown in Fig. 3.

Furthermore, with separable initial state Eq. (1) having $\phi = \frac{\pi}{2}$, the sequence $H_4H_4H_4\dots$ on 4-cycle, yields MESPS at $t = 1, 5, 9, \dots$ (here $\gamma + \phi = \frac{\pi}{2}$) with period 4, as shown in Fig. 4. Similarly, sequence $H_8H_8H_8\dots$ with $H_8 = U_8(\frac{1}{2}, 0, 0)$ yields recurrent MESPS at $t = 1, 13, 25, \dots$ with period 12

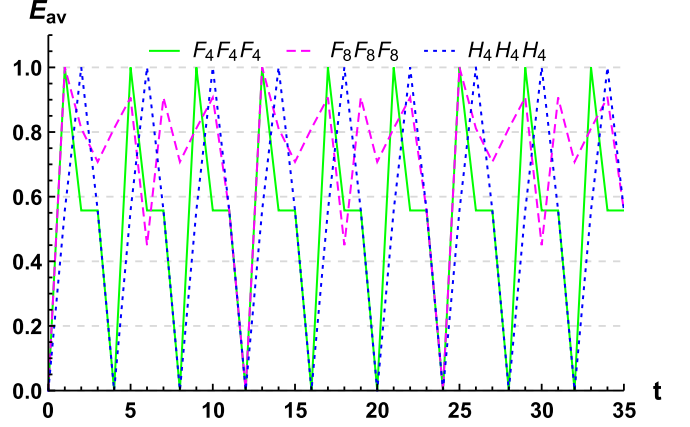


FIG. 3. E_{av} vs time steps (t) with single noninvolutory coin evolution sequences: $F_4F_4F_4\dots$ (solid green) for 4-cycle, $F_8F_8F_8\dots$ (dashed magenta) for 8-cycle, and single involutory coin evolution sequence $H_4H_4H_4\dots$ (dotted blue) for 4-cycle, for arbitrary separable initial state with $\phi = \pi$.

on 8-cycle for the same initial state, see Fig. 4. (See more examples in SM Secs. I and II [23].) The periodic behavior of $H_kH_kH_k\dots$ in generating MESPS is supported by its ordered QW dynamics on both $k = 4$ and $k = 8$ -cycles, see SM Sec. II [23] for its analytical proof. Besides, we show that more than one MESPS can also occur within the period of the QW.

Unfortunately, for both the $k = 3$ -cycle and $k = 5$ -cycle, we do not see periodic MESPS with single-coin evolution sequences. However, an arbitrary coin from Eq. (6) subject to the constraint $(\gamma + \phi) \in \{\frac{\pi}{2}, \frac{3\pi}{2}\}$ yields MESPS at $t = 1$ irrespective of whether it is an even or odd cycle, see SM Sec. II [23].

Note that a QW for a single-coin evolution sequence $A_kA_kA_k\dots$ is the simplest in terms of experimental setup, as it just uses the same coin \hat{C}_2 [Eq. (6)] at each time step [11]. In other words, the same setup will be sufficient for its realization. Thus, the above-established general framework using

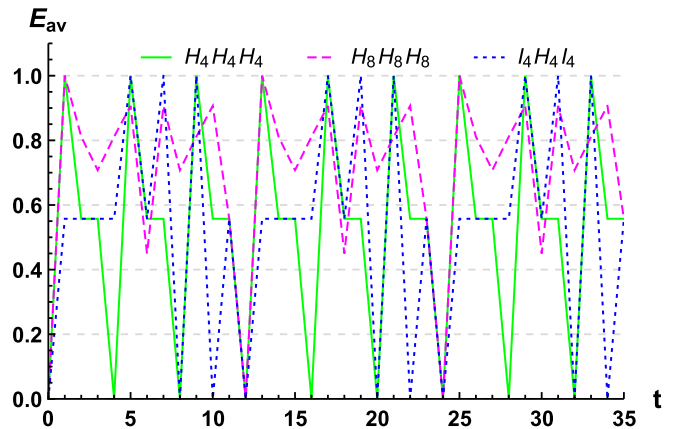


FIG. 4. E_{av} vs time steps (t) with evolution sequences $H_4H_4H_4\dots$ (solid green), $I_4H_4I_4\dots$ (dotted blue) for 4-cycle, and $H_8H_8H_8\dots$ (dashed magenta) for 8-cycle, for arbitrary separable initial state with $\phi = \frac{\pi}{2}$.

a single coin [Eq. (6)] for recurrent generation of MESPS is pivotal and resource saving.

MESPS with effective-single or two-coin evolution sequences. We execute several numerical experiments by forming multiple deterministic coin evolution sequences such as $A_k B_k A_k A_k B_k A_k \dots$, $A_k B_k A_k B_k \dots$, $A_k B_k B_k A_k B_k B_k \dots$, $A_k A_k B_k A_k A_k B_k \dots$, etc., where $A_k = U_k(\rho, \gamma, \eta) = \hat{S} \cdot [I_k \otimes \hat{C}_2(\rho, \gamma, \eta)]$ and $B_k = U_k(\rho', \gamma', \eta') = \hat{S} \cdot [I_k \otimes \hat{C}_2(\rho', \gamma', \eta')]$. Here we consider three coin operators [Eq. (2)]: Hadamard \hat{H} , Grover $\hat{X} = \hat{C}_2(\rho = 0, \gamma = 0, \eta = 0)$, and Identity $\hat{I} = \hat{C}_2(\rho = 1, \gamma, \eta \ni \gamma + \eta = \pi)$. If $\hat{C}_2 = \hat{X}$, we have evolution operator $X_k = U_k(0, 0, 0) = \hat{S} \cdot [I_k \otimes \hat{X}]$, and if $\hat{C}_2 = \hat{I}$, then evolution operator $I_k = U_k(1, 0, \pi) = \hat{S} \cdot [I_k \otimes \hat{I}]$. The primary idea behind such experiments was to reveal evolution-operator sequences involving either two coins such as $H_k H_k X_k \dots$, $H_k X_k H_k X_k \dots$, etc. or effective-single coin (i.e., I_k with either H_k or X_k) such as $I_k H_k I_k \dots$, $H_k I_k I_k \dots$, etc., which yield recurrent MESPS. We first discuss effective-single coin evolution sequences and then the two-coin evolution sequences to generate MESPS via DTQWs on either even ($k = 4$) or odd ($k \in \{3, 5\}$)-cycle. Notably, the effective-single coin evolution sequences like $I_k H_k I_k \dots$ or $H_k I_k I_k \dots$ consist of a single coin (here \hat{H}) with Identity (\hat{I}) and their experimental implementation is resource saving too, as no extra device is required for Identity coin operation, although it is slightly more complex than single-coin implementation [4].

We consider an arbitrary separable initial state Eq. (1) with $\phi = \frac{\pi}{2}$ and first discuss with the 4-cycle, the effective-single coin evolution sequences $I_4 H_4 I_4 \dots$, $H_4 I_4 I_4 \dots$ and $H_4 I_4 H_4 I_4 \dots$. We observe that the E_{av} values generated via the sequence $I_4 H_4 I_4 \dots$ follow a periodic trend, see Fig. 4. This observation is well supported by the periodic probability distribution $P(x = 0)$ for the walker position at $|0_p\rangle$, in other words, the sequence $I_4 H_4 I_4 \dots$ not only generates MESPS at $t = 5, 7, 9, 17, \dots$ with period 12 but also an ordered QW, see SM Sec. II [23]. Analytically one can also prove this by exploiting the periodicity condition, beginning with the eigenvalues of the $U_{4,1}$ block of the evolution operator $(U_4)^3$, see Eq. (3), $\lambda_{4,1}^{U_4 U_4 U_4} = \frac{1}{2} i \sqrt{\rho} e^{\frac{3}{2} i(\gamma + \eta)} (e^{-\frac{1}{2} i(\gamma + \eta)} + e^{\frac{1}{2} i(\gamma + \eta)}) (-3 + 2\rho + (e^{-i(\eta + \gamma)} + e^{i(\eta + \gamma)})\rho)$. Similarly, the $U_{4,1}$ block's eigenvalues for the sequence $I_4 H_4 I_4$ give $\lambda_{4,1}^{I_4 H_4 I_4} = \frac{i}{\sqrt{2}}$. Herein, $\lambda_{4,1}^{\tilde{U}}$ represents the sum, $\frac{\lambda_{4,1}^+ + \lambda_{4,1}^-}{2}$, for the evolution $\tilde{U} = (U_4)^3$ or $I_4 H_4 I_4$. Equating $\lambda_{4,1}^{U_4 U_4 U_4}$ with $\lambda_{4,1}^{I_4 H_4 I_4}$ for $(\gamma + \eta) = 0$, we get $\rho = \frac{2 + \sqrt{3}}{4}$, which is an exact match with ρ obtained in Ref. [9] for a periodic QW with period $N = 24$. With this description for the $I_4 H_4 I_4 \dots$ sequence giving an ordered QW, we observe that a single involutory-coin evolution sequence $C_4 C_4 C_4 \dots$ (i.e., coin $\hat{C} = \hat{C}_2(\rho = \frac{2 + \sqrt{3}}{4}, \gamma = 0, \eta = 0)$ applied at each time step) generates MESPS with period 12 at $t = 5, 17, 29, \dots$, see Fig. 5. It is another method besides Eq. (6) to obtain the condition for the single coin to give recurrent MESPS. Moreover, effective-single coin evolution sequences $H_4 I_4 I_4 \dots$ and $H_4 I_4 H_4 I_4 \dots$ yield periodic MESPS with periods 12 and 4 at time steps $t = 1, 3, 5, 13, \dots$ and $t = 1, 5, 9, \dots$, respectively (see SM Sec. II [23]).

We also observe that the two-coin evolution sequence $H_4 H_4 X_4 \dots$ gives recurrent MESPS with period 6 at

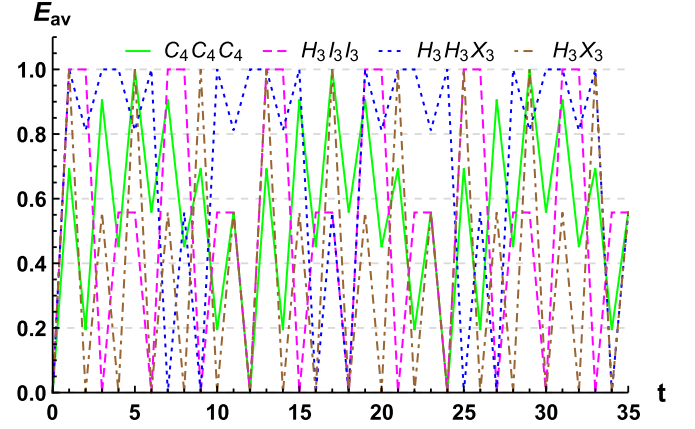


FIG. 5. E_{av} vs time steps (t) with evolution sequences: $C_4 C_4 C_4 \dots$ (solid green) for 4-cycle, and $H_3 I_3 I_3 \dots$ (dashed magenta), $H_3 H_3 X_3 \dots$ (dotted blue), $H_3 X_3 \dots$ (dot-dashed brown), for 3-cycle, for an arbitrary separable initial state with $\phi = \frac{\pi}{2}$.

$t = 1, 3, 7, 9, 13, \dots$ (proof of this periodicity is in SM Sec. II [23]), whereas the sequence $H_4 X_4 H_4 X_4 \dots$ gives recurrent MESPS with period 4 at $t = 1, 5, 9, \dots$, for 4-cycle.

Moving now to 3-cycle, the effective-single coin evolution sequence $H_3 I_3 I_3 \dots$ yields periodic MESPS with period 6 at $t = 1, 2, 7, 8, \dots$, but the sequence $I_3 H_3 I_3 \dots$ renders ordered QWs without MESPS, whereas $H_3 I_3 H_3 I_3 \dots$ renders chaotic QW with MESPS at $t = 1, 2$, see Fig. 5 and SM Sec. II [23]. However, exploiting the periodicity condition for the $H_3 I_3 I_3 \dots$ sequence does not yield a MESPS-generating single-coin evolution sequence, unlike the case for $I_4 H_4 I_4 \dots$ sequence.

From Fig. 5 we also observe that the two-coin evolution sequences $H_3 H_3 X_3 \dots$ and $H_3 X_3 H_3 X_3 \dots$ generate recurrent MESPS respectively at $t = 1, 3, 4, 6, 10, \dots$ (with period 9) and $t = 1, 5, 9, \dots$ (with period 4) via the DTQW on the 3-cycle. For proof of this periodicity and results on 5-cycle yielding recurring MESPS via effective-single and two-coin evolution sequences, see SM Sec. II [23].

Interestingly, by only employing $H_k H_k X_k \dots$, $H_k I_k I_k \dots$, and $H_k X_k H_k X_k \dots$ on a ($k = 3$)-cycle one can obtain MESPS at all time steps up to 10, whereas on a ($k = 4$)-cycle these sequences give MESPS at all odd time steps $t \leq 10$, see Fig. 5 and SM Sec. II [23]. As these sequences also beget periodic QWs, thus one obtains MESPS at larger time steps ($t > 10$) as well. Moreover, on a ($k = 5$)-cycle, just the sequences $H_k H_k X_k \dots$ and $H_k I_k I_k \dots$ generate MESPS at all time steps $t \leq 10$, see SM Secs. II and III [23].

Cryptography protocol. Periodic MESPS generation via our DTQW scheme can be exploited to design a quantum cryptographic protocol [12,24]. Herein we put forth an example with the single-coin evolution sequence $H_4 H_4 H_4 \dots$ for a 4-cycle (i.e., the Hadamard QW as shown in Fig. 4) to perform a secure encryption-decryption of a message with the following steps.

Step 1: Alice wants to send a message $m \in \{0, 1, 2, 3\}$ to Bob. Bob forms the public key as $|\psi_{pk}\rangle = A|j_p\rangle|q_c\rangle$, where $A = (H_4)^5$, $|j_p\rangle$ with $j \in \{0, 1, 2, 3\}$ and $|q_c\rangle = \cos(\frac{\theta}{2})|0_c\rangle + i \sin(\frac{\theta}{2})|1_c\rangle$, with $\theta \in [0, \pi]$, $\phi = \frac{\pi}{2}$, respectively, the

position and coin states of the quantum walker. As shown in Fig. 4, $(H_4)^{4n+1}$ with $n = 0, 1, 2, \dots$ can generate MESPS periodic in time, with $(H_4)^8 = I_8$. Thus $|\psi_{pk}\rangle$ is a MESPS. After generating this MESPS $|\psi_{pk}\rangle$, which acts as the public key, Bob sends it to Alice.

Step 2 (Encryption): Alice encodes the message via $|\psi(m)\rangle = (T_m \otimes I_c)|\psi_{pk}\rangle$, where $T_m = \sum_{i=0}^3 |((i+m) \bmod 4)_p\rangle\langle i_p|$, akin to the shift operator with $I_c = I_2$, and sends it to Bob.

Step 3 (Decryption): Bob then decrypts the message by operating $W = (H_4)^3$ from which he gets $|((j+m) \bmod 4)_p, q_c\rangle$. Bob reads $m' = (j+m) \bmod 4$ from the position ket, and from which he securely obtains Alice's message m .

The security of this MESPS-based cryptographic protocol, i.e., resilience against any eavesdropper attack like man-in-the-middle, intercept-and-resend, etc. [25], is described in SM Sec. IV [23].

Conclusions. This Letter provides a scheme to generate MESPS from separable initial quantum states via DTQWs on k cycles with $k \in \{3, 4, 5, 8\}$, with just a single coin and with both effective-single coin and two-coin evolution sequences. We established a general framework that predicts coins yielding MESPS at time step $t = 1$ via QW on any k cycle with single-coin evolution sequences from any arbitrary initial separable state (with any ϕ value subject to certain constraints) [23]. A subset of the coins yields recurrent MESPS on both 4- and 8-cycles. An analytical proof for periodic QW which supports the recurrent generation of MESPS has been established, and more than one MESPS can occur within the period of the QW, see SM Secs. I and II [23].

In addition, we show that with a 4-cycle, effective-single and two-coin evolution sequences (e.g., $I_4H_4I_4$, $H_4H_4X_4\dots$, etc.) and single-coin evolution sequence $C_4C_4C_4\dots$ (obtained from $I_4H_4I_4$), individually yield recurrent MESPS, from the initial separable state with $\phi = \frac{\pi}{2}$. Finally, with effective-single and two-coin evolution sequences, we show recurrent

MESPS generation (with the same initial state) on 3- and 5-cycles. In the 3-cycle case, the sequences $H_3I_3I_3\dots$, $H_3H_3X_3\dots$, and $H_3X_3H_3X_3\dots$ altogether give MESPS at all $t \leq 10$, whereas in the 5-cycle case, with sequences $H_5H_5X_5\dots$ and $H_5I_5I_5\dots$, one can obtain MESPS at all $t \leq 10$. In SM Sec. III [23], we summarize the evolution sequences to generate MESPS at time steps up to 10 and beyond with the cyclic graphs.

We have also outlined the steps to implement our scheme in quantum cryptography. One can experimentally implement our proposed scheme using linear optical elements such as half-wave plates (HWPs), quarter-wave plates (QWPs), and polarizing beam splitters (PBSs), along with a fast switching electro-optical modulator (EOM), wherein the photon's polarization degree of freedom encodes the coin state with the position state is encoded into different time bins of the photon [11,19]. Evaluating the entanglement entropy requires postprocessing measurements like average polarizations of the photon by proper arrangement of an HWP and QWP [19,26].

A comparison of our work with other relevant works (DTQWs on 1D line) [3,4,16,21,27] can be found in SM Sec. V [23]. Apart from opening an avenue for MESPS generation, our Letter significantly outperforms other schemes in model simplicity and resource-saving architecture and periodically yields MESPS at both small and large time steps. We provide a PYTHON code for numerical experiments in SM Sec. VI [23].

Our presented work significantly contributes towards state-of-art controlled (maximal) entanglement generation protocols, a fundamental resource in quantum computing, teleportation, and cryptography, and a prerequisite for quantum-information-processing tasks.

Acknowledgment. C.B. would like to thank the Science and Engineering Research Board (SERB) for funding under a Core Research Grant titled Josephson junctions with strained Dirac materials and their application in quantum information processing," Grant No. CRG/2019/006258.

-
- [1] S. Azzini, S. Mazzucchi, V. Moretti, D. Pastorello, and L. Pavesi, Single-particle entanglement, *Adv. Quantum Technol.* **3**, 2000014 (2020).
- [2] S. Kochen and E. P. Specker, The Problem of Hidden Variables in Quantum Mechanics, *J. Math. Mech.* **17**, 59 (1967).
- [3] A. Gratsea, M. Lewenstein, and A. Dauphin, Generation of hybrid maximally entangled states in a one-dimensional quantum walk, *Quantum Sci. Technol.* **5**, 025002 (2020).
- [4] X.-X. Fang, K. An, B.-T. Zhang, B. C. Sanders, and H. Lu, Maximal coin-position entanglement generation in a quantum walk for the third step and beyond regardless of the initial state, *Phys. Rev. A* **107**, 012433 (2023).
- [5] C. H. Bennett and G. Brassard, Quantum cryptography: Public key distribution and coin tossing, *Theor. Comput. Sci.* **560**, 7 (2014).
- [6] C. Vitelli, N. Spagnolo, F. Sciarrino, E. Santamato, and L. Marrucci, Joining the quantum state of two photons into one, Research in optical sciences, OSA Technical Digest, Paper QW3B.2 (Optical Society of America, Washington, DC, 2014).
- [7] G. Zhu, L. Xiao, B. Huo, and P. Xue, Photonic discrete-time quantum walks, *Chin. Opt. Lett.* **18**, 052701 (2020).
- [8] Y. Aharonov, L. Davidovich, and N. Zagury, Quantum random walks, *Phys. Rev. A* **48**, 1687 (1993).
- [9] P. R. Dukes, Quantum state revivals in quantum walks on cycles, *Results Phys.* **4**, 189 (2014).
- [10] B. Tregenna, W. Flanagan, R. Maile, and V. Kendon, Controlling discrete quantum walks coins and initial states, *New J. Phys.* **5**, 83 (2003).
- [11] Z.-H. Bian, J. Li, X. Zhan, J. Twamley, and P. Xue, Experimental implementation of a quantum walk on a circle with single photons, *Phys. Rev. A* **95**, 052338 (2017).
- [12] A. Panda and C. Benjamin, Order from chaos in quantum walks on cyclic graphs, *Phys. Rev. A* **104**, 012204 (2021).
- [13] G. P. Harmer and D. Abbott, Losing strategies can win by Parrondo's paradox, *Nature (London)* **402**, 864 (1999).
- [14] S. S. Panda, P. A. Ameen Yasir, and C. M. Chandrashekar, Quantum direct communication protocol using recurrence in k -cycle quantum walks, *Phys. Rev. A* **107**, 022611 (2023).

- [15] B. Whaley and G. Milburn, Focus on coherent control of complex quantum systems, *New J. Phys.* **17**, 100202 (2015).
- [16] D. K. Panda, B. Varun Govind, and C. Benjamin, Generating highly entangled states via discrete-time quantum walks with Parrondo sequences, *Physica A* **608**, 128256 (2022).
- [17] S. Li, H. Yan, Y. He, and H. Wang, Experimentally feasible generation protocol for polarized hybrid entanglement, *Phys. Rev. A* **98**, 022334 (2018).
- [18] C. M. Chandrashekar, Disorder induced localization and enhancement of entanglement in one and two-dimensional quantum walks, [arXiv:1212.5984](https://arxiv.org/abs/1212.5984).
- [19] R. Vieira, E. P. M. Amorim, and G. Rigolin, Dynamically Disordered Quantum Walk as a Maximal Entanglement Generator, *Phys. Rev. Lett.* **111**, 180503 (2013).
- [20] R. Vieira, E. P. M. Amorim, and G. Rigolin, Entangling power of disordered quantum walks, *Phys. Rev. A* **89**, 042307 (2014).
- [21] A. Gratsea, F. Metz, and T. Busch, Universal and optimal coin sequences for high entanglement generation in 1D discrete time quantum walks, *J. Phys. A: Math. Theor.* **53**, 445306 (2020).
- [22] D. Janzing, Entropy of entanglement, in *Compendium of Quantum Physics*, edited by D. Greenberger, K. Hentschel, F. Weinert (Springer, Berlin, Heidelberg, 2009).
- [23] See Supplemental Material at <http://link.aps.org/supplemental/10.1103/PhysRevA.108.L020401> for more details, which includes Refs. [3,4,9,16,21,24,25,27].
- [24] C. Vlachou, J. Rodrigues, P. Mateus, N. Paunković, and A. Souto, Quantum walk public-key cryptographic system, *Int. J. Quantum Inf.* **13**, 1550050 (2015).
- [25] V. Gaur, D. Mehra, A. Aggarwal, R. Kumari, and S. Rawat, *Quantum Key Distribution: Attacks and Solutions*, Proceedings of the International Conference on Innovative Computing & Communications (ICICC) (2020).
- [26] A. Peres, *Quantum Theory: Concepts and Methods* (Kluwer Academic, New York, 2002).
- [27] R. Zhang, R. Yang, J. Guo, C.-W. Sun, J.-C. Duan, H. Zhou, Z. Xie, P. Xu, Y.-X. Gong, and S.-N. Zhu, Maximal coin-walker entanglement in a ballistic quantum walk, *Phys. Rev. A* **105**, 042216 (2022).